EGU2011-2395, A83: Session GD2.4/SM4.1/TS10.2: The Lithosphere-Asthenosphere Boundary (LAB) Dilemma

Institute for Energy Technology

PHYSICS OF GEOLOGICAL PROCESSES

A phase change model for (one of) the LAB(s)

Nina S.C. Simon [a), b), c)]
a) Institute for Energy Technology, Kjeller, Norway; nina.simon@ife.no
b) Dep. of Earth Sciences, University of Bergen, Bergen, Norway
c) Physics of Geological Processes, University of Oslo, Oslo, Norway

BACKGROUND

1. Based on a large seismic dataset, Rychert and Shearer (*1*) globally mapped a sharp interface at a depth that varies with tectonic environment and lies at 95 km underneath Precambrian shields and at about 70 km underneath ocean islands (Fig. 1). A drop in seismic velocities around these depths is pertinent in a large number of geophysical studies.
2. The garnet-in reaction (simplified: olivine + Al-rich pyroxenes + spinel = olivine + Al-poor pyroxene + garnet) takes place in the mantle at pressures corresponding to 40-90 km, depending on temperature and degree of depletion (Cr/Al ratio) of peridotite (Fig. 2).
3. Recent experimental results (e.g. (*2*, *3*)) indicate that the solubility of hydrogen in pyroxenes depends on the Al content of the pyroxenes.

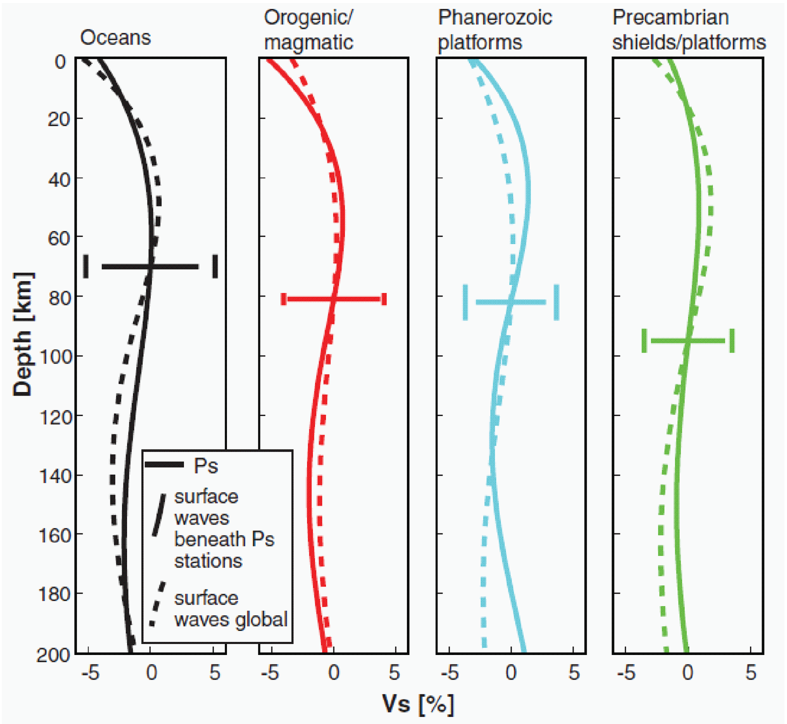

Fig. 1: Results of Ps mapping from (*1*). Depths of the discontinuity varies with tectonic setting.

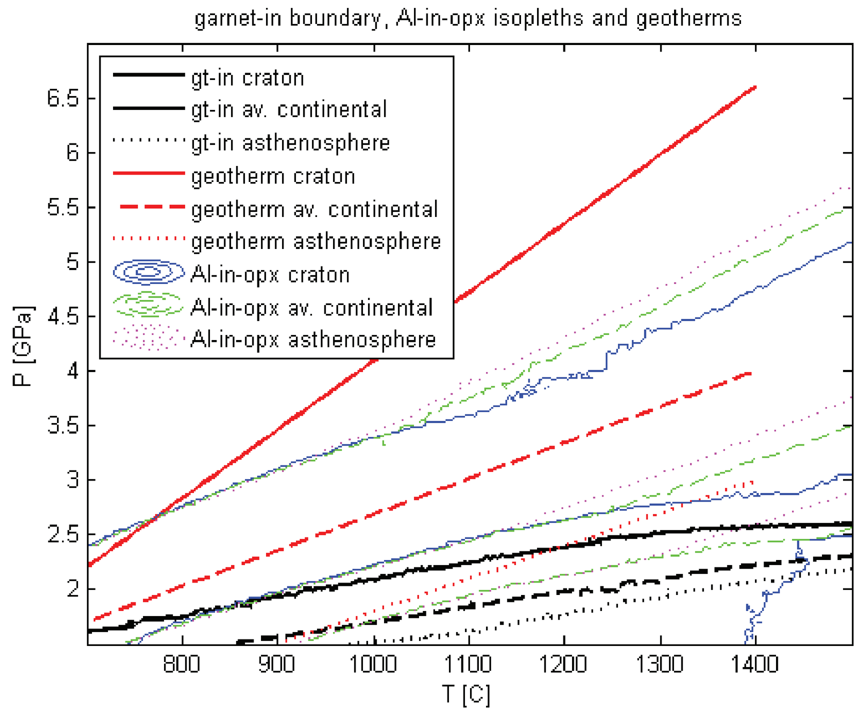

Fig. 2: The red lines are typical mantle geotherms for the three different tectonic settings selected here. Also shown in black are the garnet-in boundaries (1 wt% garnet) for the three different compositions given in Table 1. The thin lines are Al-in-opx isoleths for 1, 3 and 5 wt% Al_2O_3 in orthopyroxene (see legend).

	Ronda (Frey et al., 1985)		
wt%	R893	R25	R243
SiO_2	43,01	44,43	45,12
Cr_2O_3	0,29	0,45	0,37
Al_2O_3	0,89	2,40	3,64
FeO(tot)	7,99	8,12	8,30
MgO	47,17	42,09	39,09
CaO	0,78	2,61	3,24
Na_2O	0,03	0,16	0,32
Total	100,16	100,26	100,08
Mg#	0,91	0,90	0,89

Table 1: Mantle peridotite compositions from Ronda. R893, R25 and R243 are chosen as representative for strongly refractory cratonic, average continental, and fertile (asthenospheric) mantle, respectively. Bulk water content for all compositions was set to 50 ppm.

RESULTS

I calculated mineral modes and compositions for 3 representative bulk compositions (Table 1) using Perple_X07 (*4*). I then obtained the hydrogen contents of olivine and pyroxenes using Al-dependent partition coefficients (modified from (*3*)) and a fixed bulk water content of 50 ppm (Fig. 3). Effective viscosities for olivine dislocation creep for the different olivine water contents are then calculated (*5*) and compared to viscosities at a constant olivine water content (Fig. 4). Finally, I extracted the olivine hydrogen contents and the viscosities along three different typical geotherms (Fig. 5 and 6).

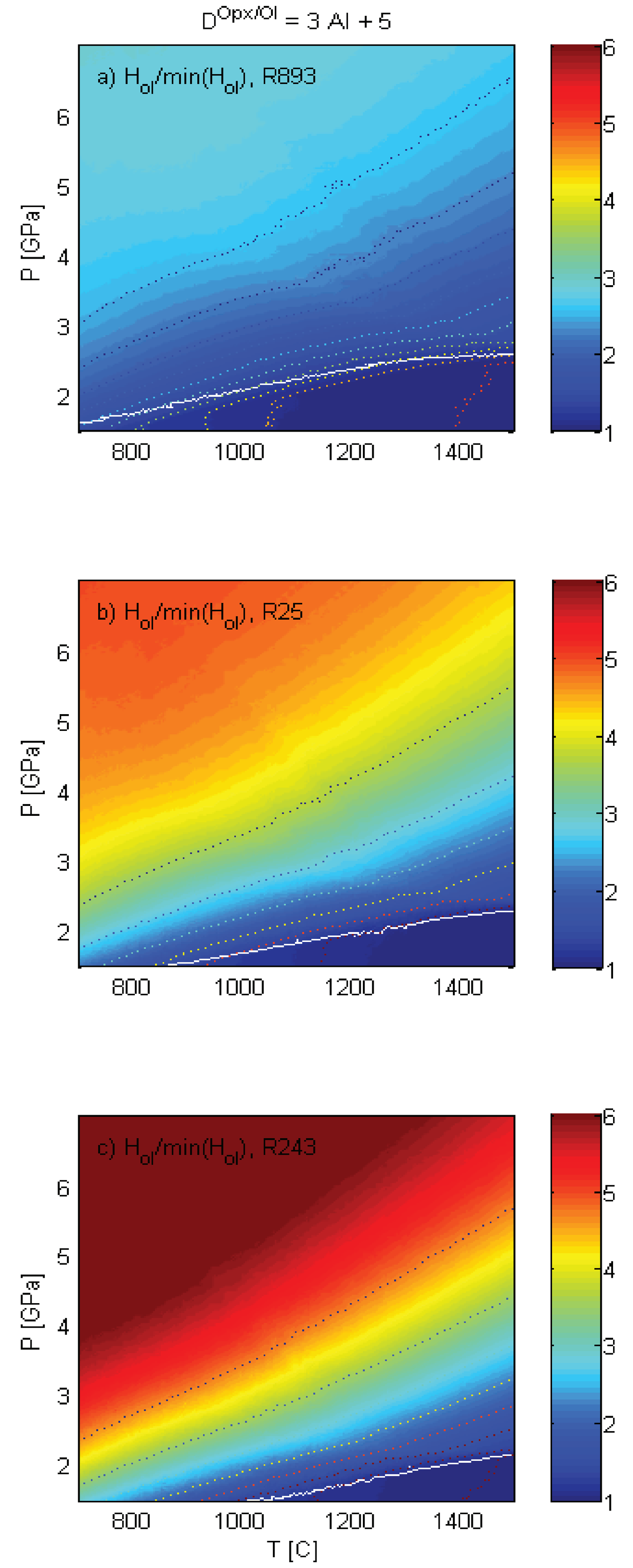

Fig. 3: Variation in olivine water content due to modal variations and the dependence of the partition coefficient between olivine and pyroxenes on the Al-content in pyroxenes. H(ol) decreases with T and increases with P. Also shown are contours for 1 wt% modal garnet (white) and the 1, 3 and 5 wt% Al_2O_3 isopleths in opx (dotted).

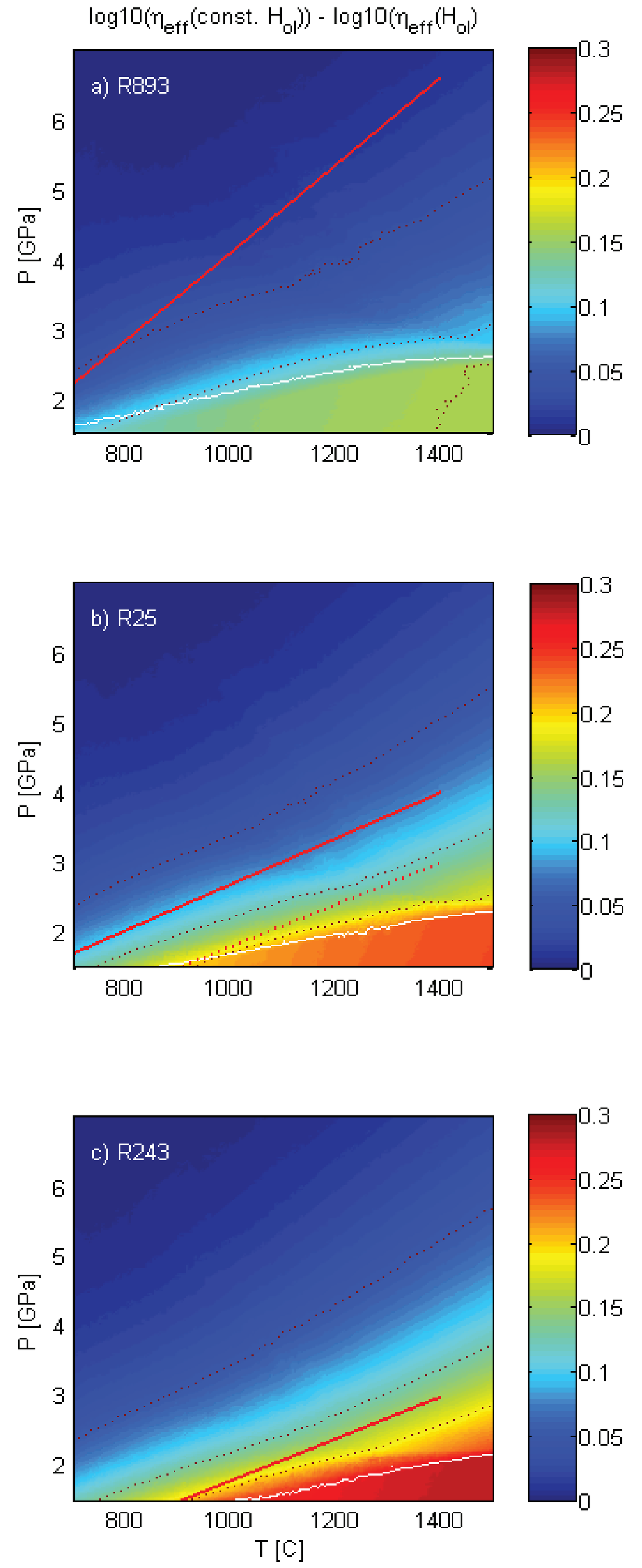

Fig. 4: Effect of the changes in olivine hydration on the effective viscosity (in log10 units). The effect is small (max. 0.25 log units) compared to the exponential influence of temperature, especially since the largest variations are not cut by typical geotherms (they would be by the adiabat, however). Dehydration of olivine at high T counteracts the weakening effect of temperature. Mantle geotherms plotted in red, garnet-in boundaries in white and Al-in-opx isoleths as dotted lines.

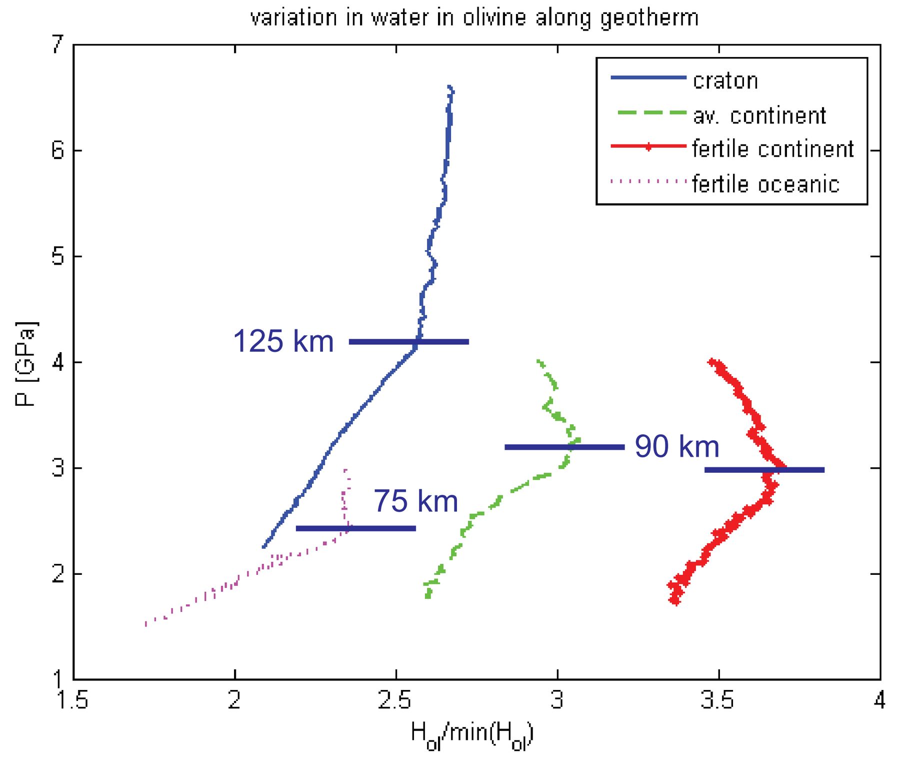

Fig. 5: Variation of normalized water content in olivine along the mantle geotherms shown in Figs. 1 and 4. 'Fertile continent' refers to the most fertile (astenospheric) bulk composition along the intermediate geotherm. Note that the depth of the change in slope varies with tectonic setting not only as a consequence of different P-T, but also bulk composition. The kink is deepest in cold, cratonic, refractory mantle and shallowest in hot and fertile young lithosphere.

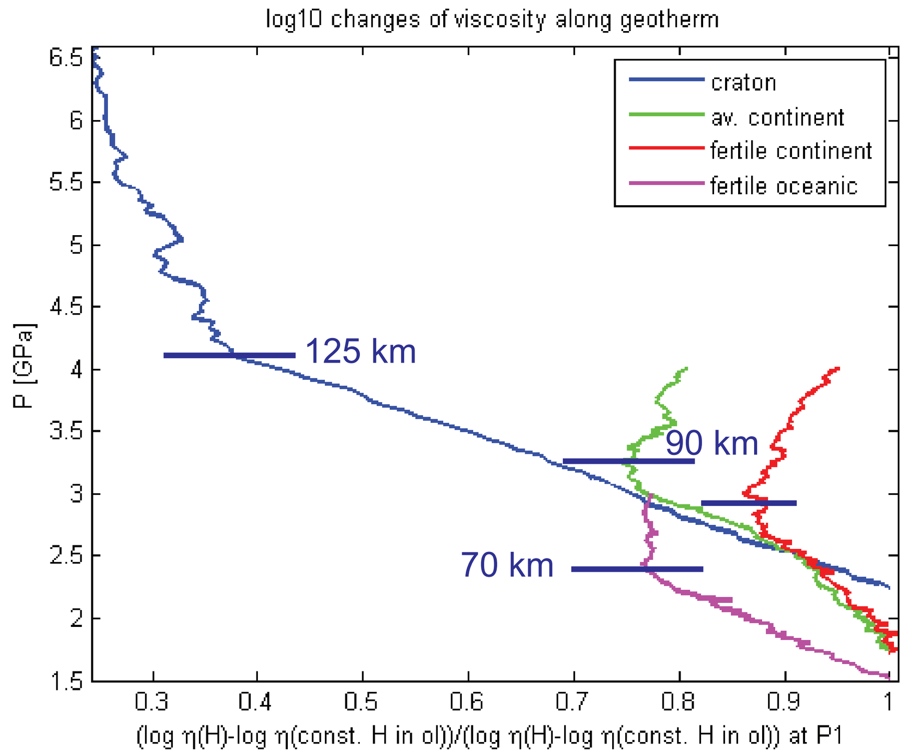

Fig. 6: Viscosity variations along the geotherm corrected for the effect of pressure and temperature, to only show the effect of changes in water content in olivine. Difference normalized to difference at start of geotherm (see Fig. 1). At depth, viscosity is relatively constant and starts to increase above a certain level, indicated by the thick blue lines labled with approximate depth. The green and red lines illustrate the effect of composition since the temperature at a given pressure is the same. The relative effect on mantle viscosity is largest refractory, cold mantle, but stretched over a large depth interval, whereas the transition is mcuh sharper for fertile mantle and a hot geotherm.

DISCUSSION AND CONCLUSIONS

The release of hydrogen from pyroxenes results in an increase in hydrogen in olivine (Fig. 3). The depth and sharpness of the increase in hydrogen in olivine, along the geotherms and for the bulk mantle compositions typical for the different tectonic settings, fit very well with the geophysical data (Fig. 5). The magnitude of this variation on olivine hydration is independent of initial peridotite composition and bulk water content. The effect of this hydrogen variation on viscosity, however, is minor in comparison to the exponential influence of pressure and temperature (Fig. 4 and 6). However, uncertainties in the olivine flow law are large and there may be other effects of the garnet-in boundary and the associated hydrogen re-distribution that may explain the discontinuity imaged by geophysical methods, in particular underneath old shields where alternative explanations fail. The phase change mechanism operates globally in all peridotitic mantle. The depth of the boundary depends on degree of melt depletion (and temperature) and is predicted to be shallowest in fertile lithosphere and deepest in refractory cratonic lithosphere, consistent with the observations.

REFERENCES

(*1*) Rychert, C.A. and Shearer, P.M., 2009. A Global View of the Lithosphere-Asthenosphere Boundary. Science, 324(5926): 495-498.
(*2*) Mierdel, K., et al., 2007. Water Solubility in Aluminous Orthopyroxene and the Origin of Earth's Asthenosphere. Science, 315(5810): 364-368.
(*3*) Tenner, T.J., Hirschmann, M.M., Withers, A.C. and Hervig, R.L., 2009. Hydrogen partitioning between nominally anhydrous upper mantle minerals and melt between 3 and 5 GPa and applications to hydrous peridotite partial melting. Chemical Geology, 262(1-2): 42-56.
(*4*) Connolly, J.A.D., 2005. Computation of phase equilibria by linear programming: A tool for geodynamic modeling and its application to subduction zone decarbonation. Earth Planet Sci Let, 236(1-2): 524-541.